Fractal-Microcavity Composites: Giant Optical Responses

Won-Tae Kim[1], Vladimir P. Safonov[2], Vladimir P. Drachev[3], Viktor A. Podolskiy[1], Vladimir M. Shalaev[4], and Robert L. Armstrong[1]

[1] Department of Physics, New Mexico State University, Las Cruces, NM 88003, USA
[2] Institute of Automation and Electrometry, Novosibirsk 630090, Russia
[3] Institute of Semiconductor Physics, Novosibirsk 630090, Russia
[4] School of Electrical and Computer Engineering, Purdue University, West Lafayette, IN 47907-1285, USA
shalaev@purdue.edu

Abstract. A novel class of materials, fractal-microcavity composites, that provides unprecented enhancement of optical responses is developed. These composites combine the energy-concentrating effects due to localization of optical excitations in fractals with the strong morphology-dependent resonances (MDRs) of dielectric microcavities. Optical excitation of fractal-microcavity composites may result in truly gargantuan local fields. By coupling the localized plasmon modes in fractals with MDRs, strong lasing and nonlinear Raman scattering can be obtained at low light intensities. This allows developing efficient microlasers and makes Raman and hyper-Raman spectroscopy a powerful analytical tool for detecting and characterizing a small number of, or even single molecules.

Advances in science and technology often result from the development of new or improved materials. For example, the arrival of advanced optical media has heralded companion advances in photonics and in laser and detector technology. In this contribution, we demonstrate that nanostructured materials fabricated in our laboratory exhibit dramatically superior optical performance characteristics, foreshadowing great promise for both fundamental and applied studies.

1 Introduction

Since the advent of the laser nearly 40 years ago, its unique characteristics have been used to generate a variety of linear and, especially, nonlinear optical emissions such as stimulated scattering and harmonic generation. The initiation of nonlinear emissions typically requires intense pumping sources so that, in practice, emissions are observed only for powerful laser sources whose intensity exceeds some threshold value. The threshold depends on many factors, notably, the quality (Q) factor of the optical resonator containing the emitting medium and the strength of the nonlinear interaction, expressed in terms of a nonlinear susceptibility.

V. M. Shalaev (Ed.): Optical Properties of Nanostructured Random Media,
Topics Appl. Phys. **82**, 149–167 (2002)

Given the dependence of the threshold pump intensity on medium parameters, it is natural to inquire whether media exist for which initiation of nonlinear emissions occurs for threshold pump intensities dramatically lower than for conventional media. We suggest that a defining characteristic of such media is the existence of greatly enhanced local fields; here, we quantify this concept in terms of an "enhancement factor" given by the magnitude of the ratio of the local to the incident electric field amplitudes. If the enhancement factor is sufficiently large, even extremely weak pump beams will drive local field amplitudes above the threshold required for a particular nonlinear process with the result that emission generated by this process is excited in the medium.

The media of interest here are composites consisting of colloidal silver fractal aggregates and dielectric microcavities. The colloidal silver particles have an average diameter of the order of 10 nm. Using well-established chemical or other fabrication methods, fractal aggregation of the particles may be achieved, and the resulting aggregates, typically comprising 10^2–10^3 silver particles, have dimensions of approximately 1 μm. Composites are formed when aggregates are seeded into a dielectric microcavity; in our experiments, this consisted of a hollow quartz tube of outer diameter 1 mm and inner diameter 0.7 mm. As we shall see, since each component possesses a large enhancement factor and the enhancement factor of the composite depends multiplicatively on the enhancement factors of the individual components, the enhancement factor of the composite can become enormous. Because of this gigantic enhancement, the lasing threshold can decrease significantly, and the efficiency of various optical processes can dramatically increase. In particular, we show here that record-high enhancement for Raman and hyper-Raman scattering can be achieved in the fractal-microcavity composites making possible nonlinear Raman spectroscopy at very low light intensities.

In the remainder of this contribution, we first review the important properties of fractal aggregates and dielectric microcavities and discuss fabrication of the composites. We follow this by a discussion of selected experiments performed in our laboratory that exhibit the remarkable optical characteristics of the composites.

2 Optical Properties of the Composites

The giant enhancement of optical responses in metal nanocomposites and thin metallic films containing nanoscale surface features has been intensively studied in recent years [1,2]. This enhancement is associated with the excitation of surface plasmons, collective electromagnetic modes whose characteristics depend strongly on the geometric structure of the metallic component of the medium.

2.1 Fractal Silver Aggregates

Nanocomposites often are scale-invariant, and their structure is characterized by fractal geometry [3]. Since fractal objects do not possess translational invariance, they cannot transmit the running waves that are characteristic of homogeneous media. Rather, collective optical excitations in fractals result from near-field multiple scattering within subwavelength regions of the fractal medium; hence, optical excitations, such as surface plasmons, are often spatially localized in fractals [2,4]. The localization is inhomogeneous in the sense that, at any wavelength, modes of different coherence radii are excited [5]. This localization leads to the presence of nanometer-scale spatial regions of high local electrical fields, "hot" spots, and accordingly, to significant enhancement for a variety of optical processes, such as Raman scattering, four-wave mixing, the quadratic electro-optical effect, and nonlinear absorption and refraction [2,6].

The symmetry of fractals is distinctly different from that of continuous media, for example, crystals or gases. Continuous media possess translational invariance so that the medium has the same appearance (at least statistically) at different spatial locations. However, fractal media possess the distinct symmetry of scale invariance so that a fractal has the same appearance (again, at least statistically) when viewed on different spatial scales. These fundamentally different symmetries strongly influence the nature of their resonant excitations. Resonance modes of continuous media are typically delocalized; moreover, medium constituents within a given region absorb light at approximately equal rates and possess approximately equal excitation amplitudes. In contrast, resonance modes of fractal media are spatially localized within subwavelength regions, "hot spots", and the excitation of constituents within these hot spots can greatly exceed those of constituents at other spatial locations [2].

The localization of optical excitations in fractals within small, subwavelength, spatial regions results in extremely large enhancement factors and the corresponding enhancement of many optical effects such as Rayleigh, Raman, and nonlinear light scattering [2]. The enhancement is especially large for nonlinear processes since, in this case, the intensity depends on the power of the enhanced local field. For example, consider degenerate four-wave mixing (DFWM), where both the driving field and the nonlinear amplitude are enhanced. Theory predicts [2] a large enhancement, $G \propto Q^6$, confirmed experimentally [4], where an enhancement factor of the order of 10^6 occurs upon fractal aggregation of colloidal silver nanoparticles.

2.2 Microcavities

Microcavities, such as liquid or solid microspheres and microcylinders, are a second essential component of a composite. Microcavities exhibit a rich spectrum of electromagnetic resonances [7], termed morphology-dependent

resonances or MDRs. These resonances, which may have extremely high quality factors ($Q = 10^3$–10^9), result from confinement of the radiation within a microcavity by total internal reflection. Light emitted or scattered in a microcavity may couple to the high-Q MDRs lying within its spectral bandwidth, leading to enhancement of both spontaneous and stimulated optical emissions. For example, enhanced fluorescence emission from an organic dye-doped cylindrical or spherical microcavity occurs when either the laser pump or the fluorescence (or both) couple to microcavity MDRs [8]. Moreover, the increased feedback produced by MDRs is sufficient to obtain laser emission from a dye-doped microdroplet under both CW [9] and pulsed [10] laser excitation, with the threshold CW pump intensity three orders of magnitude lower than that of a conventional dye laser in an external cavity. Lasing emission from a microcavity doped with two fluorescent species (a dye-doped sol and a liquid dye) occurs via enhanced radiative (MDR) and nonradiative (Forster) energy transfer [11]. The existence of high-Q microcavity modes is also responsible for numerous stimulated nonlinear effects, including stimulated Raman and Rayleigh-wing scattering and four-wave parametric oscillation under moderate intensity CW excitation [12]. The microcavities used to obtain the results discussed in this contribution consist of hollow quartz tubes (approximately 1 mm o.d., 0.7 mm i.d.) in which we place silver colloids or colloidal silver fractal aggregates for spectroscopic study. These microcavities possess resonance modes having Qs of the order of 10^3–10^5.

With increasing pump power, even in the absence of fractal silver or colloidal silver material in the microcavity, resonance enhancement provided by the MDRs may drive the emission into the nonlinear regime. However, with the introduction of such material, SERS- and fractal aggregate-related enhancement effects may be many orders of magnitude greater; hence, numerous nonlinear processes may be observed, even at extremely low concentrations of the emitting species and extremely low pump power.

2.3 Composites

To perform optical experiments with fractal-microcavity composites, the initial problem is to be able to fabricate them reliably. This process, in turn, requires fabrication of fractal aggregates, microcavities, and subsequent coupling of the two. Fractal aggregates have been fabricated by other groups [1], and we too developed fabrication capabilities in our laboratory. Normally, the fractal fabrication process consists of two distinct phases: the growth of colloidal particles and the formation of fractal aggregates of these particles. We have used two chemical methods to grow colloidal silver particles, the Lee–Meisel method [13] and Creighton's method [1]. Although both methods result in the formation of colloidal solutions of silver particles with diameters of the order of 10 nm, our experiments show that the Lee–Meisel method results in colloidal solutions possessing a somewhat higher silver concentration; this, in turn, results in more intense optical emissions during spectroscopic

investigations. Hence, in the remainder of this contribution, most of our results for chemically produced fractals were obtained using the Lee–Meisel method.

The formation of the colloidal silver solution is the most delicate step in the chemical fractal fabrication process. Careful control of both the constituent concentrations and the ambient temperature is needed to obtain uniform size distribution of silver particles; this, in turn, strongly influences the optical properties of aggregates formed from the particles. Once the colloidal solution is obtained, fractal aggregation may readily be induced by the addition of a suitable organic acid; we used fumaric acid in our experiments. The acid pH is a convenient parameter that may be used to control the aggregation rate; the lower the pH, the faster the aggregation rate. Fractal-microcavity composites are formed by the simple expedient of dipping the open end of the quartz microcavity into the fractal solution where capillary action readily introduces the fractal solution into the microcavity.

Two nonchemical methods were also used to fabricate fractal aggregates: the laser ablation technique and the photoaggregation method. In the laser ablation method, a vacuum chamber containing a silver target is first evacuated and subsequently backfilled to a selected pressure with an inert gas such as helium. Irradiating the target by a high-power laser (entering through a window in the vacuum chamber) causes ablation of silver; in our experiments, we used a Nd:YAG laser to accomplish this. As a function of gas pressure and pump power, first silver monomers, and subsequently silver fractal aggregates, are formed in the ambient gas above the target; this material is subsequently deposited on a substrate inside the chamber. This method provided us with fractal aggregate colloidal silver samples primarily used in experiments designed to increase our understanding of fractal media.

The photoaggregation method, first suggested in [14], was further developed during a series of our experiments discussed later in this contribution. These experiments clearly indicated that irradiation of a colloidal solution by an external pump laser results in the formation of fractal aggregates. Subsequent experiments employing scanning electron microscopy revealed that the aggregation rate as well as the maximum size of the resulting fractal aggregates exhibits a strong dependence on both the wavelength and power of the pump laser.

We conclude this section by noting that there are several reasons for the giant enhancement factors exhibited by fractal-microcavity composites. First, local-field amplitudes are increased in the neighborhood of individual silver monomers via coupling to the localized surface plasmon resonances of fractal aggregates. Second, seeding the aggregates into microcavities further increases the local fields because of light trapping by microcavity resonance modes [7]. Finally, evidence will be presented here that chemical modification of adsorbed molecules may occur resulting in the presence of a sizable chemical enhancement factor [1].

For the spectral emissions reported in this contribution, our results indicate that the enhancement factor may be enormous, exceeding 10^{26} in one of our experiments. Such gigantic enhancement factors foreshadow many other results, including the detection of emissions from single molecules and nanoparticles.

3 Lasing in Fractal-Microcavity Composites

The initial optical study of fractal-microcavity media was an investigation of lasing [15]. Fractal aggregate optical excitations may be concentrated in regions smaller than the diffraction limit of conventional optics, resulting in large local fields. Seeding the aggregates into microcavities further increases the local fields because of light trapping by microcavity resonance modes. These composites possess unique optical characteristics, including extremely large probabilities of radiative processes. In our experiments, we observed lasing at extremely low threshold pump intensities, well below 1 mW (for some experimental trials, below 50 μW), and dramatically enhanced Raman scattering.

Strong existing evidence suggests that fractal nanocomposites and microcavity resonators individually result in large enhancements of optical emissions. We demonstrate that huge, multiplicative enhancement factors are obtained under the simultaneous, combined action of these two resonant processes when the emitting species is adsorbed onto fractal aggregates contained within high-Q microcavities. We found that doping a dye solution inside a microcavity containing fractal silver aggregates results in a giant enhancement of the efficiency of lasing and nonlinear Raman scattering. Note that, although colloidal Ag aggregates introduce absorption and, hence, linear losses inside the microresonator, at the same time they increase the efficiency of dye excitation and emission. We believe that results discussed in this contribution demonstrate the unique potential of such devices in the development of ultra low threshold microlasers, nonlinear optical devices for photonics, as well as new opportunities for micro analysis, including spectroscopy of single molecules.

Colloidal silver solutions, prepared using the Lee–Meisel method [13], result in the formation of silver nanoparticles (monomers) with an average diameter of 25 nm. Addition of an organic acid (e.g., 0.03 M saturated fumaric acid) to the monomer solution promotes the aggregation of colloidal nanoparticles into fractal clusters, containing, typically, 10^3 monomers. Electron microscopic analysis of the aggregates (see inset in Fig. 1a) reveals that they possess a fractal structure with the fractal dimension D $\approx$ 1.8 characteristic of the cluster–cluster aggregation of monomer particles.

Extinction spectra of nonaggregated silver colloids in the visible region of the spectrum exhibit a single resonance feature centered at 420 nm and width 80 nm; this peak is due to the surface plasmon excitation in single silver

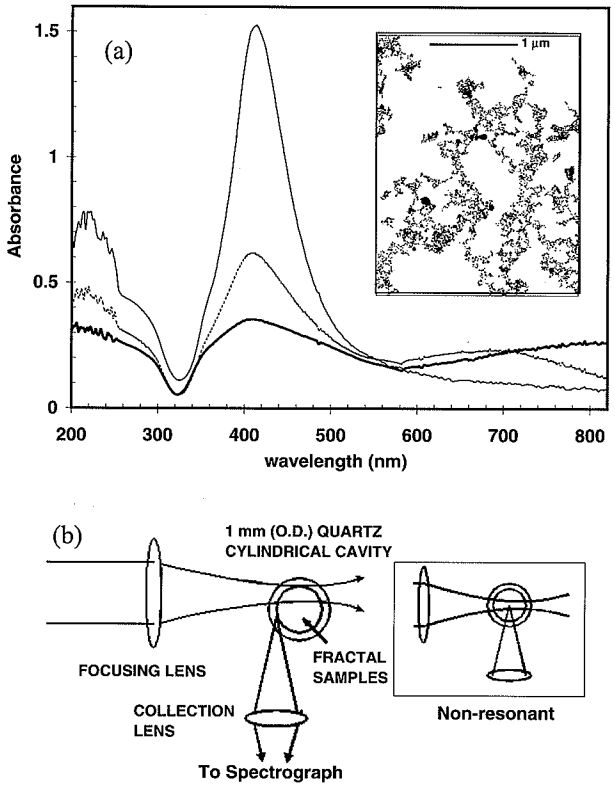

Fig. 1. **(a)** Absorption spectra of silver colloids in different aggregated states (from 1 cm path length cuvettes) and TEM image of fractal aggregates. With an increase of the aggregation degree, the peak at 420 nm decreases and the broad long-wavelength wing becomes stronger. **(b)** Experimental illumination scheme

nanoparticles. Aggregation leads to the appearance of a broad wing extending toward the long-wavelength part of the spectrum. Enhanced extinction in the long-wavelength region (see Fig. 1a) is a consequence of induced high-Q optical modes in metal fractal aggregates [2].

Lasing experiments were performed using Rhodamine 6G (R6G) dye. A small amount of a parent solution of 10^{-4} M R6G in methanol was added to the colloidal silver solution; the resulting dye concentrations ranged from 10^{-8} to 10^{-5} M. Cylindrical microcavities were fabricated from cylindrical quartz tubes (diameter, 700 μm, outer diameter, 1000 μm), with the dye/colloidal solution placed within the tube.

A 10-mW CW Ar-ion laser (λ = 514.5 nm) and a 0.75 mW CW green He–Ne laser (λ = 543.5 nm) were used as pumping sources in these experiments. The pump beam (approximately 2 mm in diameter) was focused into the tube by a 75-mm focal length lens; focal plane beam diameters were 70 μm

and 35 μm for Ar- and He–Ne lasers, respectively. Pump beam polarization was vertical (along the axis of the tube), and output radiation was collected at 90° to the incident radiation, as shown in Fig. 1b; different configurations shown in Fig. 1b were used when MDRs were (were not) excited in the cylindrical microcavity. Spectroscopic measurements were performed using a CCD camera mounted to a SpectraPro-300i spectrograph; an 1800/mm grating provided an instrumental spectral resolution of 0.028 nm (full width at half maximum, FWHM).

Elastic scattering of a laser beam passed through the outer edge of the empty cylindrical tube exhibited a well-defined, MDR angular structure; alternatively, when the beam is passed through the inner edge of the empty tube, the intensity of the MDR peaks is significantly reduced. However, filling the tube with a colloidal solution again resulted in strong elastic scattering with a clearly resolved MDR angular structure. Most of our experiments were performed using this illumination geometry. Our observations imply that elastic scattering by fractal aggregates and monomers contributes to output coupling of radiation from microcavity MDRs. Scattering, together with absorption, decreases the quality factor Q of the cavity modes according to $Q^{-1} = Q_{\mathrm{a}}^{-1} + Q_{\mathrm{sv}}^{-1} + Q_{\mathrm{ss}}^{-1}$, where Q_{a}^{-1}, Q_{sv}^{-1}, and Q_{ss}^{-1} are losses due to absorption, volume scattering, and surface scattering, respectively [6]. (Diffraction losses are negligible in our case.) If colloidal aggregates are present in the microcavity, the volume absorption is the most important loss mechanism. The measured absorption coefficient $\alpha = 5\,\mathrm{cm}^{-1}$ at $\lambda = 543.5\,\mathrm{nm}$, so that $Q_{\mathrm{a}} = 2\pi n/\alpha\lambda_{\mathrm{L}} = 3.4 \times 10^4$, where $n = 1.46$ is the refractive index. The measured scattering loss, $Q_{\mathrm{sv}}^{-1} + Q_{\mathrm{ss}}^{-1}$, is smaller than Q_{a}^{-1} by, at least, one order of magnitude, implying that scattering may be regarded in our experiments primarily as an output-coupling mechanism for microcavity radiation.

Figure 2 contrasts the luminescent spectrum of a 5×10^{-7} M aqueous dye solution in a microcavity with and without the presence of fractal silver aggregates. Without aggregates, a weak, broad luminescent band is observed with a maximum at $\lambda = 560\,\mathrm{nm}$ and a FWHM of 30 nm for $\lambda_{\mathrm{L}} = 514.5\,\mathrm{nm}$ excitation; the lower trace in Fig. 2 shows the central portion of this spectrum, and the inset provides an expanded view. In the inset, representative groupings of small amplitude peaks may be seen corresponding to luminescent emission coupled to microcavity MDRs. The intermode spacing between these peaks is approximately $\Delta\lambda \approx 0.066\,\mathrm{nm}$. This spacing is slightly smaller than the theoretical intermode spacing of $\Delta\lambda = (\lambda^2/2\pi a)[(n^2-1)^{-1/2}\tan^{-1}(n^2-1)^{1/2}] \approx 0.076\,\mathrm{nm}$, calculated for a quartz microcavity of radius $a = 0.5\,\mathrm{mm}$ and refractive index $n \approx 1.46$. The spectral widths of the peaks were limited by our instrumental resolution.

In the presence of fractal aggregates, the luminescent intensity and spectrum are changed dramatically. Figure 2 illustrates the huge increase in MDR peak intensities within a narrow spectral region centered near $\lambda = 561\,\mathrm{nm}$ with a bandwidth of approximately 3 nm for the tube containing the Ag-

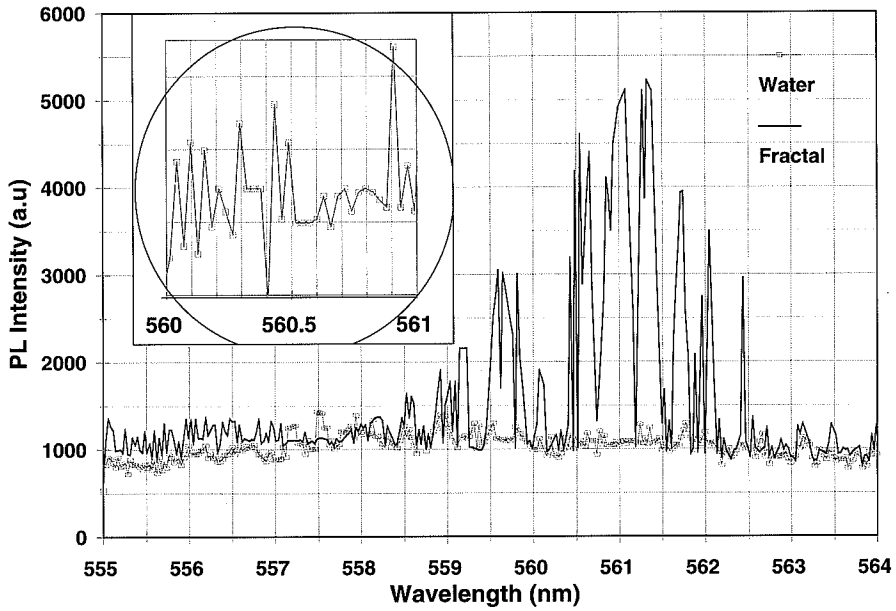

Fig. 2. Luminescent spectrum of 5×10^{-7} M R6G dye solution in microcavity, with (*heavy line*, neutral density o. d. = 5 filters are used) and without (*circles, thin line*) fractals, for $\lambda_{\mathrm{L}} = 514.5\,\mathrm{nm}$, CW Ar laser excitation. *Inset* gives detail of spectrum without fractals showing typical mode structure

R6G composite. Closely spaced but spectrally distinct modes in this region have intermode spacings essentially identical to those for the aggregate-free spectra discussed in the preceding paragraph. The measured value of a single peak FWHM, $\delta\lambda = 0.04\,\mathrm{nm}$ (it is close to our instrumental width), allows us to estimate a lower bound for the quality factors, $Q > \lambda/\delta\lambda = 1.5 \times 10^4$. This lower bound value is consistent with the previous estimate of $Q \cong 3.1 \times 10^4$.

Analogous enhanced emission spectra from a dye/fractal/microcavity system are observed under He–Ne laser excitation. Huge MDR peaks are centered near $\lambda = 600\,\mathrm{nm}$ in this case. The narrowing of the emission spectrum (from 30 nm to 3 nm) is characteristic of laser action. To test this point, we studied the emission intensity of different spectral components as a function of the pump intensity. It was found that this dependence is linear for low excitation intensities for all components. However, when the pump intensity exceeds a certain critical value in the range between 20 and $50\,\mathrm{W/cm}^2$, some peaks grow dramatically, exhibiting a lasing threshold dependence (Fig. 3). The threshold power for $\lambda_{\mathrm{L}} = 543.5\,\mathrm{nm}$ He–Ne laser excitation is as small as $2 \times 10^{-4}\,\mathrm{W}$.

The enhanced emission was found confined within an approximately 50-μm region of the tube in a vertical direction, which contained the incident

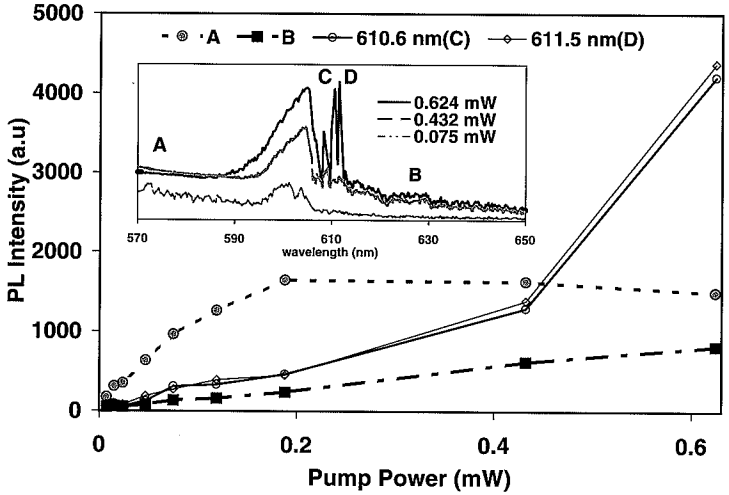

Fig. 3. Nonlinear dependence of luminescent peak intensity on pump power. A typical luminescent spectrum near 572 nm is shown as the *dashed line*. Peaks in the presence of fractals are shown as the *solid lines*

pump light; moreover, emission from this region exhibits angular patterns characteristic of microcavity MDRs.

Thus, the spectral, threshold, and spatial dependencies confirm the laser nature of the observed emission. It is noteworthy that the R6G concentration was only 5×10^{-7} M in these experiments, three orders of magnitude lower than that for conventional dye lasers with an external cavity and for a microdroplet laser without fractal silver aggregates [12]. In our experiments, the minimum R6G concentration that results in lasing can be as low as 10^{-8} M. These findings suggest that the lasing effect is due to dye molecules adsorbed on the surface of silver aggregates. This conclusion is also supported by the fact that increasing the R6G concentration to 10^{-5} M does not result in additional growth of the lasing peak intensities compared with the 5×10^{-7} M concentration; the additional dye concentration is apparently not adsorbed onto the silver particles, but remains in solution as free molecules, where it does not effectively contribute to the enhanced lasing effect. We conclude that for our composites, the effect of increasing local pump and emitted fields losses is connected with optical absorption by fractals and nonradiative quenching of excitation. Possibly, saturation of fractal absorption facilitates the lasing. The problem of luminescent excitation and amplification (and a possible role of cooperative radiative effects) for molecules adsorbed onto a metal fractal requires further studies.

We note that during the course of the lasing experiments, we also observed pump-induced photoaggregation, reported earlier in [14]. Our experiments carried out to investigate the spectroscopic consequences of the photoaggregation effect had dramatic results. A system consisting of an approximately 10^{-8} M R6G dye solution together with unaggregated colloidal silver particles was placed within a microcavity and irradiated by a 543.5-nm, CW, He–Ne pump laser with a power of approximately 50 μW. For more than 20 min, only very weak luminescent emission was observed from the microcavity. Then, during a very brief period (a minute or two), intense laser emission became visible, coupled to a small number of microcavity MDRs. This emission persisted for a time of the order of 1 h before disappearing. At that time, examination revealed that no fractal material remained in solution within the microcavity; the fractal aggregates presumably grew large enough that they precipitated out. Corroborative experiments using the electron microscope confirmed that, for irradiation with this pump laser, significant aggregation occurred on a timescale of the order of 15–30 min, and sedimentation of the fractals occurred within an hour or so. We interpret these novel findings as direct evidence for the existence of enhancement due to fractal resonance modes. A pump power of 50 μW corresponds to below-threshold conditions for the dye-colloid-microcavity system; however, if aggregation occurs, thereby increasing the enhancement because of the contribution of fractal resonance modes, the system will be driven above threshold (for the same pump power). Our experiments strongly suggest that photoaggregation has resulted in this increased enhancement. Another important factor in the observed time-dependent effect can be related to the light-induced pulling of fractals into the high-intensity area associated with the whispering gallery modes of the microcavity.

To summarize this section, results reported here promise an advance in the design of micro/nanolasers, operating on a small number of, or even on individual, molecules adsorbed on metal nanostructures within a micro/nanocavity, as well as offering the possibility of combining surface-enhanced radiative processes and high-Q morphology-dependent resonances in microcavities.

4 Ultra-Broadband 200–800 nm Light Emission

The Raman effect has long been used in spectroscopic analysis. However, until recently, Raman methods were seldom the method of choice due to the extremely small Raman scattering (RS) cross section, which is of the order 10^{-29} cm^2. Nonlinear Raman spectroscopy is, in principle, a useful analytical tool, but requires intense laser pumping sources which may introduce unwanted side effects such as photo-induced damage and plasma breakdown. However, even with the use of intense pumping sources, nonlinear Raman processes may still be extremely weak. Consider hyper-Raman scattering (HRS), where the Raman emission is excited by harmonics of the pump laser. The ratio of HRS to ordinary Raman scattering intensities depends on the incident laser pump intensity and is typically $10^{-8} - 10^{-9}$ for pump intensities of the order 10^7 W/cm^2 [16]. A significant increase in the RS intensity results

from the mechanism of surface-enhanced RS (SERS), where samples of interest are adsorbed onto nanoscale roughened metal surfaces or nanostructured metal colloids. SERS, which has proven to be a very sensitive spectroscopic method with high molecular specificity, increases the average Raman intensity by a factor of $\sim 10^6$ [1]. Hyper-Raman scattering from adsorbed molecules also benefits from surface enhancement [17,18], which generally includes both enhancements of local electromagnetic fields and the resonant character of nonlinear processes resulting from the charge-transfer band [17]. Under the resonance conditions, hyper-Raman processes could be accompanied by cascade, step-like processes, in which the intermediate and upper energy levels are first populated and then the radiative decay occurs from these states. Since one may not distinguish these processes, we call them nonlinear resonance scattering processes. However, to be observable, it still requires very large intensities, $\sim 10^6\,\mathrm{W/cm^2}$ or larger. Here, we present evidence that far greater enhancement of Raman and may be achieved at low pump intensity in fractal-microcavity composite media. With the aid of these composites, nonlinear Raman spectroscopy can become an efficient analytical tool for detecting and characterizing a small number of, or even single molecules.

We have observed enhanced light emission on the metal surface in the stokes and anti-stokes sides of a spectrum from such media using a CW He–Ne pump laser with a power level as low as 1 mW (the corresponding intensity is as low as $20\,\mathrm{W/cm^2}$). To obtain the enhanced light emission spectra, fractal-microcavity composites were irradiated by a Spectra-Physics 632.8 nm laser with a maximum power of approximately 15 mW. The He–Ne laser was focused near the rim of the microcavity in a plane perpendicular to its axis; this geometry insures efficient coupling of the pump light to microcavity MDRs (see Fig. 1b). The He–Ne pump excites Raman and luminescent emissions from Ag-particles/ sodium citrate complex, present in concentrations of 5×10^{-4} M as a by-product of fractal preparation. The role of each component of this complex is under study. These emissions, likewise coupled to MDRs, emanate from the microcavity rim where a portion of the light is gathered by a collecting lens and input to an Acton imaging spectrograph fitted with either a 300- or an 1800-groove/mm holographic grating. Spectrally analysed emissions are recorded with the aid of a Princeton Instruments two-dimensional CCD detector.

To avoid possible spectral contamination by laser plasma lines, a laser filter was placed before the sample. A blocking notch filter was inserted after the sample to minimize the amount of stray light at the pump wavelength reaching the CCD. Composite spectra were obtained by superposing eight individual overlapping spectral regions from the 200–800 nm band, using long- or short-pass filters placed after the sample to isolate each region. Individual spectra were combined by matching the relative values of peak intensities in the overlapped portions accounting for the spectral sensitivity of the CCD. This procedure eliminates possible spectral contamination by grating ghosts

or overlapping diffraction orders; thus, there is no doubt in the credibility of the measured spectra. However, we should note weak reproducibility of the spectra described here and in Section 3, which could be a result of the short-time stability of the used colloid. Figure 4a shows a low-resolution spectrum obtained using a 300 grooves/mm grating. The spectra obtained are extremely broadband, spanning a range from at least 200 to 800 nm; spectra

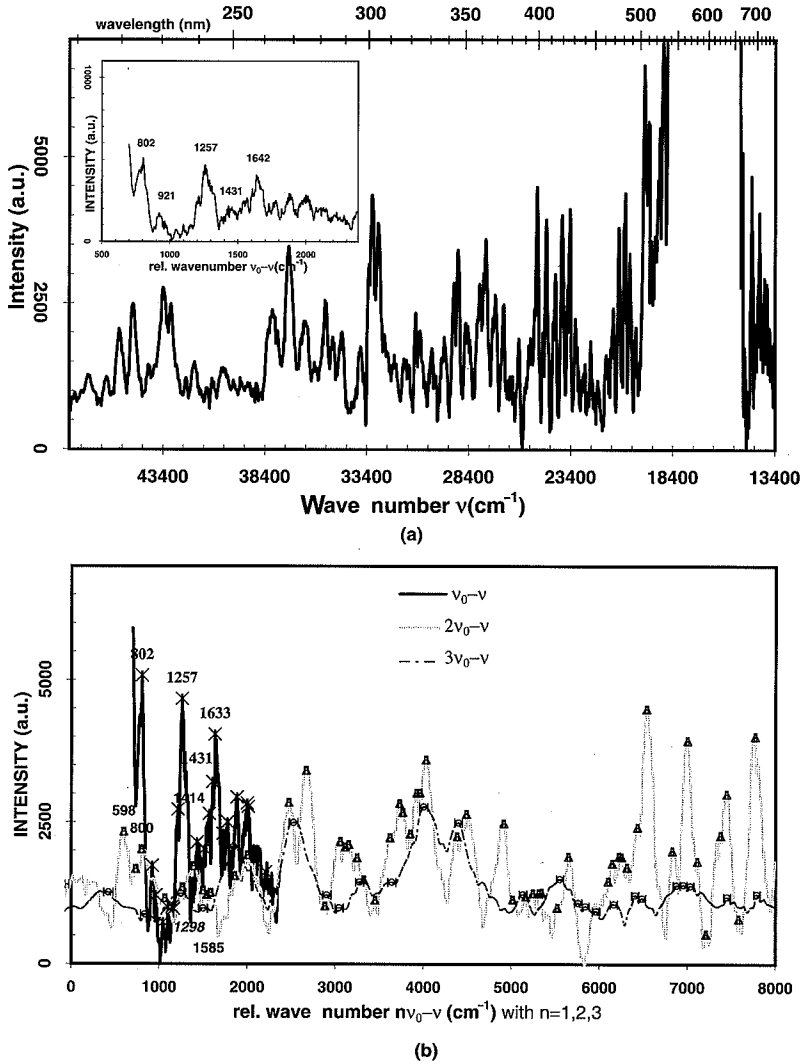

Fig. 4. (a) Emission spectrum of the composite and Raman Stokes spectrum of sodium citrate (inset). (b) Stokes sides of the spectra with respect to ν_0, $2\nu_0$, and $3\nu_0$

were not recorded outside of this range because of the degraded response of the spectrometer and the CCD. The spectrum on the anti-Stokes side consists of several groups of well-resolved lines in the ν_0 to $2\nu_0$ region with the spectral resolution from 5 to 20 cm^{-1}. In the $2\nu_0$ to $3\nu_0$ region, CCD "pixel" errors are larger, 47 cm^{-1}, and spectral structures are poorly resolved or unresolved. The features in this spectrum will be discussed below. The insert displays the Stokes-side spectrum, which contains Raman peaks and a broad emission band.

To estimate the contribution of hyper-Raman scattering from pure molecular transitions to the anti-Stokes spectrum, we should specifically compare the emission spectrum with Raman peak positions, and estimate the hyper-Raman/Raman intensity ratio.

According to previous studies[21,22], SERS spectra from sodium citrate on Carey-Lea citrate-stabilized silver hydrosol show a weak band near 650–660 cm^{-1}, no band near 1640–1660 cm^{-1}, and a dominant band at 1400 cm^{-1}. As described above, we prepared silver sol using the Lee-Meisel method with addition of NaCl. In this case, sodium citrate, a salt of a propanetricarboxylic acid $C_6H_8O_7$, exhibits a modified SERS spectrum (see Fig. 4a insert) characteristic of some carboxylic acids, such as substituted acetic [23] and formic acids [24]. The spectral signature of the modified spectrum includes a reduced intensity of the COO^- vibration near 1410 cm^{-1} (the dominant band in bulk spectra) and increased intensity of Raman bands near 1640 cm^{-1} (C=0 stretch), with the ratio of intensities strongly depending on adsorption details. Previous studies of SERS spectra of different carboxylic acids [21,22,23,24,25,26] exhibit slightly different spectra for the same adsorbate and equivalent SERS spectra for different adsorbates. Explanations for the modified spectrum include geometric orientation effects of the adsorbate with respect to the metal surface [23,26] and chemical transformation during formation of the adsorbate-metal complex [24], so that the spectra depend on sol preparation and age. The presence of Cl^- results in an intense 1636 cm^{-1} band and an unobservable 1400 cm^{-1} band, indicating that COO^- has been desorbed from the silver surface and the molecules are adsorbed mainly via the OH group [25].

Summarizing, the comparison of spectral lines near $2\nu_0$ with Raman peaks near ν_0 (see Fig. 4b) reveal that only a small number can be interpreted as hyper-Raman scattering from adsorbate molecules: specifically, two peaks (at 800 and 933 cm^{-1}) have shifts from $2\nu_0$ approximately equal to the SERS shifts 807 and 921 cm^{-1}; in addition, a number of other peaks may be regarded as overtones of the Raman fundamentals (e.g., $2 \times 1256\,cm^{-1}$, $2 \times 1642\,cm^{-1}$, $3 \times 1256\,cm^{-1}$). Thus, although we can identify a fraction of peaks as resulting from surface-enhanced Raman and hyper-Raman scattering, many peaks in the broad-band spectrum may not be attributed to either Raman or hyper-Raman scattering from adsorbate molecules and should be treated as nonlinear resonant scattering resulting from multi-photon-pumped

luminescence from discrete states of metal particles or adsorbate-molecule/metal-particle complexes [26]. This conclusion is also supported by comparison of the measured ratio of the RS/nonlinear scattering intensities and theoretical estimates for hyper-Raman scattering discussed below.

The measured enhancement factor for Raman scattering, $G^{(RS)}$, is defined as the product of two measured RS intensity ratios. The first ratio comes from comparison of RS in citrate adsorbed on fractal aggregates and in concentrated sodium citrate solution without colloid, $I_f/I_w \sim 10^5$–10^6; and the second one comes from comparison of RS from fractal solutions with and without a microcavity, $I_{f-mc}/I_f \sim 10^4$. The resulting factor $G^{(RS)} \sim 10^9$–10^{10}, exceeds by up to four orders of magnitude the *average* (macroscopic) RS enhancement on rough metal surfaces and colloidal aggregates.

With the proven fact that the RS enhancement in fractals is concentrated in nanometer-sized hot spots where it exceeds the average RS-enhancement by up to six orders of magnitude [2], we conclude that the *local* RS-enhancement in the hot spots of the fractal-microcavity composites can be as large as 10^{15}–10^{16} [15]. These enhancement factors exceed the local enhancements for single molecule SERS ($10^{12} \sim 10^{15}$) observed in [19,20]. Therefore, we expect that placing fractal nanostructures in a microcavity will facilitate new possibilities for optical microanalysis and studies of lasing and nonlinear optical effects in single molecules.

Following Reference [17], the ratio of hyper-Raman/Raman intensity may be estimated from the ratio of RS and HRS intensities in bulk solution, which is $I_{HRS}/I_{RS} \sim 10^{-14}$–$10^{-15}$ for a pump intensity, $I \sim 50\,W/cm^2$, used in our experiments. For pure molecular transitions, the cross-sections are assumed to be unchanged; hence, this ratio may increase only as a result of the local field enhancement in fractal-microcavity composites.

In general, the intensity for n-photon pumped HRS can be approximated by $I_{n\mathrm{HRS}} = \sigma_{n\mathrm{HRS}} I^n G^{(n)}_{\mathrm{fract}}\, g^{(n)}_{\mathrm{cav}}$, where $\sigma_{n\mathrm{HRS}}$ is the n-photon-pumped HRS cross section, I is the intensity of the pump at the fundamental frequency, $G^{(n)}_{\mathrm{fract}}$ is the local-field HRS enhancement factor in fractals, and $g^{(n)}_{\mathrm{cav}}$ is the local-field HRS enhancement of the cavity's MDRs. The case of $n = 1$ corresponds to conventional RS so that $G^{(1)}_{\mathrm{fract}} = G^{(\mathrm{RS})}_{\mathrm{fract}}$; the cases of $n = 2$ and $n = 3$ correspond to two- and three-photon pumped HRS, respectively. MDR and fractal enhancements are decoupled in this approximation.

The fractal-field enhancement $G^{(n)}_{\mathrm{fract}}$ for HRS is defined through the averaging of a ratio (raised to a proper power) of the local and external fields. Following the general approach described in [2], we found an analytical expression for $G^{(n)}_{\mathrm{fract}}$ in terms of $X(\omega)$ and $\delta(\omega)$, which are the known functions of the wavelength and defined via $-[\alpha_0]^{-1} = Z = X + i\delta$, where α_0 is the polarizability of individual spherical monomers forming the fractal. The corresponding formulas are as follows. For conventional RS, with a relatively small Stokes shift (so that $X(\omega_s) \approx X(\omega) = X$), $G^{(\mathrm{RS})}_{\mathrm{fract}} \approx |Z/\delta|^4\, \delta \mathrm{Im}\, \alpha\,(X)$.

For RS ($n = 1$) with a large shift and for HRS, $G^{(n)}_{\text{fract}} \approx \left[|Z/\delta|^{2n}\,\delta \text{Im}\,\alpha\,(X)\right] \times \left[|Z_s/\delta_s|^2\,\delta_s Im\alpha\,(X_s)\right]$, where $X_s = X(\omega_s)$. In these formulas, $\text{Im}\,\alpha\,(X)$ is the average absorption by fractals (Fig. 1a) calculated in [2]. As seen in Fig. 5, the formulas above are in good accord with our simulations based on numerical solution of the coupled-dipole equations in fractals [2]. Both theory and simulations show strong enhancement for RS, especially, for HRS, that increases toward the infrared, where quality factors of fractal plasmon modes are much larger [2].

The microcavity enhancement $g^{(n)}_{\text{cav}}$ depends on whether the fundamental and Stokes waves couple to the MDRs of the cavity. It can range from $g^{(n)}_{\text{cav}} \sim Q^n_\lambda$ (only the fundamental wave is coupled to the MDRs) and $g^{(n)}_{\text{cav}} \sim Q_{\lambda_s}$ (only the Stokes wave is coupled to MDRs) up to $g^{(n)}_{\text{cav}} \sim Q^n_\lambda Q_{\lambda_s}$, when both waves are coupled to MDRs (Q_λ and Q_{λ_s} are the cavity quality factors at λ and λ_s). However, if none of the waves couples to MDRs, $g^{(n)}_{\text{cav}} \sim 1$. Typical quality factors for our microcavities range from 10^4 to 10^5. Thus, even if we assume that the cavity enhancement for the two-photon pumped HRS is close to its maximum, $g^{(2)}_{\text{cav}} \sim Q^2_\lambda Q_{\lambda_s} \sim 10^{15}$, and multiply it by the fractal enhancement $G^{(2)}_{\text{fract}} \sim 10^6$ at $\lambda = 632\,\text{nm}$, the resultant factor is still much less than experimentally observed. Since the experimental spectra contain many anti-Stokes emission peaks whose intensities are approximately equal to the Stokes Raman peak intensities, we conclude that they cannot arise from hyper-Raman scattering from pure molecular transitions. We believe that there is an additional source of strong enhancement in our composites, which we assume to be the chemical enhancement. We also note that to

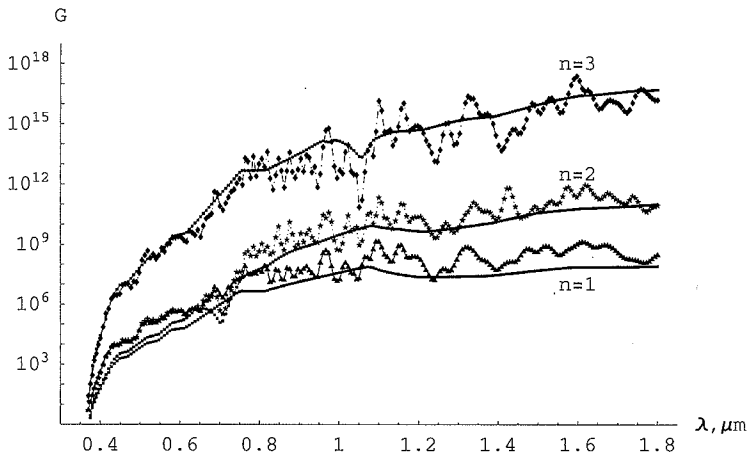

Fig. 5. Theoretical and simulated SERS and SEHRS fractal-field enhancement factors; $G^{(n)}_{\text{fract}}$, in silver fractals

describe properly this enhancement one needs to take into consideration the discrete metal-particle states, as was pointed out in[26].

Chemical enhancement results in modification of the cross section $\sigma_{n\text{HRS}}$, occurring when adsorbates bind strongly to the SEHRS-active surface so that Raman emission does not arise from the adsorbate alone, but rather from an adsorbate–surface complex (e.g., see [28,29,30]). These new charge-transfer states can contribute resonantly to the Raman and hyper-Raman cross section of the surface complex, greatly increasing its magnitude.

The fractal plasmon modes can play an important role in the chemical enhancement, as they do in electromagnetic (EM) enhancement. For example, energy transfer, which is facilitated by the Ag_n clusters, can occur between fractal plasmon modes and vibronic excitations of molecules adsorbed onto the metal surface. Plasmons can decay into single electron excitations that lead to the resonant enhancement of RS and HRS enhancement [31]. The process can also be mediated by so-called ballistic electrons arising through the plasmon excitations (see [32] and references therein).

We believe that the giant nonlinear emission observed is due to combined contributions from the electromagnetic and chemical enhancements, both strongly benefiting from the fractal plasmon modes.

The dramatic EM enhancement in fractal-microcavity composites and the resonant character of Raman processes resulting from the charge-transfer bands can result in an unusual dependence of the observed emission on pump intensity because of saturation effects. For example, if a two-photon transition is saturated so that the upper level population does not further increase with intensity, then, the intensity dependence for three-photon-pumped HRS is quasi-linear rather than I^3 because the hyper-Raman process, in this case, can be roughly thought of as a conventional Raman process from the upper level of the two-photon transition. Similarly, if the one-photon transition is saturated, then two-photon-pumped HRS should have a quasi-linear dependence. Our experimental studies of the intensity dependence (not shown) support this conclusion. The measurements indicate that with an increase in the laser pump power, the intensity dependence (initially nonlinear) quickly becomes quasi-linear for pump power above 2 mW. The saturation means that the HRS cross section becomes intensity-dependent. We stress that the lasing effect [15] observed in the same system also provides strong evidence for saturation at low pump power. Finally, we note that at saturation, one may not distinguish between truly multiphoton processes (such as conventional HRS) and cascade, step-like processes, in which the upper energy level is first populated and then a Raman process occurs from that state [33].

Thus, in fractal-microcavity composites, nonlinear Raman spectroscopy becomes possible at low light intensities that makes it a powerful analytical tool for detecting and characterizing molecules.

Because of giant multiplicative enhancement of optical responses in fractal-microcavity composites, we can also expect generation of higher harmon-

ics and cascaded Stokes and anti-Stokes spectral components when the higher vibrational levels are populated. The experiments described above indicate that there is efficient generation of new spectral components covering a very large spectral interval from the near-infrared to the ultraviolet, when the fractal-microcavity composite is irradiated by a low-power He–Ne laser. We speculate that various optical nonlinearities, such as harmonic generation, hyper-Raman and cascaded Stokes and anti-Stokes Raman scattering and their phase-matched counterpart, coherent anti-Stokes Raman (and hyper-Raman) scattering (CARS and CAHRS), can be dramatically enhanced in the composites and generated simultaneously, even at very moderate pump power.

It is interesting to note that the enhancement is expected to increase with the order of the optical nonlinearity because, in this case, the process is proportional to the enhanced local field raised to a greater power; in other words, the larger the nonlinearity, the stronger the enhancement. Under these circumstances, different order optical nonlinearities can coexist and compete with each other, leading to a number of very interesting complex phenomena involving high nonlinearities and feedback, such as optical multistability, optical chaos, and optical self-organization and pattern formation.

Acknowledgments

This work was supported in part by National Science Foundation (DMR-98101183 and DMR-0071901), Petropleum Research Fund (35028-AC5), Civilian Research and Development Foundation (RE1-2229), Army Research Office (DAAG55-98-1-0425 and DAAD19-01-1-0682), and NASA under Grants NAG 8-1710 and NCC-1-01049.

References

1. K. Chang, T. E. Furtak (Eds.), *Surface Enhanced Raman Scattering* (Plenum, New York 1982); M. Moskovits, Rev. Mod. Phys. **57**, 783 (1985)
2. V. M. Shalaev, *Nonlinear Optics of Random Media: Fractal Composites and Metal-Dielectric Films* (Springer, Berlin, Heidelberg 2000)
3. B. B. Mandelbrot, *The Fractal Geometry of Nature* (Freeman, San Francisco 1982); A. L. Barbasi, H. E. Stanley, *Fractal Concepts in Surface Growth*, (Cambridge University Press, Cambridge 1995); R. Jullien, R. Botet, *Aggregation and Fractal Aggregates*, (World Scientific, Singapore 1987); F. Family, T. Viscek, *Dynamics of Fractal Surfaces* (World Scientific, Singapore 1990)
4. V. M. Shalaev, M. I. Stockman, Sov. Phys. JETP **65**, 287 (1987); A. V. Butenko, V. M. Shalaev, M. I. Stockman, Sov. Phys. JETP **67**, 60 (1988); S. G. Rautian, V. P. Safonov, P. A. Chubakov, V. M. Shalaev, M. I. Stockman, JETP Lett. **47**, 243 (1988); V. A. Markel, L. S. Muratov, M. I. Stockman, T. F. George, Phys. Rev. B **43**, 8183 (1991)
5. M. I. Stockman, L. N. Pandey, T. F. George, Phys. Rev. B **53**, 2183 (1996); M. I. Stockman, Phys. Rev. E **56**, 6494 (1997); Phys. Rev. Lett. **79**, 4562 (1997)

6. V. M. Shalaev, Phys. Reports **272**, 61 (1996); V. A. Markel, V. M. Shalaev, E. B. Stechel, W. Kim, R. L. Armstrong, Phys. Rev. B **53**, 2425 (1996); V. M. Shalaev, E. Y. Poliakov, V. A. Markel, Phys. Rev. B **53**, 2437 (1996); Yu. E. Danilova, V. P. Drachev, S. V. Perminov, V. P. Safonov, Bull. Russian Acad. Sci. Phys. 60, 342 (1996); Ibid. 374; Yu. E. Danilova, N. N. Lepeshkin, S. G. Rautian, V. P. Safonov, Physica A **241**, 231 (1997)
7. R. K. Chang, A. J. Campillo (Eds.), *Optical Processes in Microcavities* (World Scientific, Singapore 1996)
8. J. F. Owen, P. W. Barber, P. B. Dorain, R. K. Chang, Phys. Rev. Lett. **47**, 1075 (1981)
9. H.-M. Tzeng, K. F. Wall, M. B. Long, R. K. Chang, Opt. Lett. **9**, 499 (1984)
10. A. Biswas, H. Latifi, R. L. Armstrong, R. G. Pinnick, Opt. Lett. **14**, 214 (1988)
11. R. L. Armstrong, J. G. Xie, T. E. Ruekgauer, R. G. Pinnick, Opt. Lett. **17**, 943 (1992)
12. M. B. Lin, A. J. Campillo, Phys. Rev. Lett **73**, 2440 (1994)
13. P. C. Lee, D. Meisel, J. Phys. Chem. **86**, 3391 (1982)
14. S. V. Karpov, A. K. Popov, and V. V. Slabko, JETP Lett. **66**, 106 (1997)
15. W. Kim, V. P. Safonov, V. M. Shalaev, R. L. Armstrong, Phys. Rev. Lett. **82**, 4811–4814 (1999)
16. L. D. Ziegler, J. Raman Spectrosc. **21**,769–779 (1990)
17. J. T. Golab et al., J. Chem. Phys. **81**, 7942 (1988)
18. K. Kneipp et al., Chem. Phys. **247**, 155 (1999)
19. K. Kneipp K. et al., Phys. Rev. Lett. **78**, 1667 (1997)
20. S. Nie, S. R. Emory, Science **275**, 1102 (1997)
21. M. Kerker, O. Siiman, L. A. Bumm, D.-S. Wang, Appl. Opt.,19, 3253–3255 (1980)
22. O. Siiman, L. A. Bumm, R. Callaghan, C. G. Blatchford, M. Kerker, J. Phys. Chem., 87, 1014–1023 (1983)
23. S. Kai, W. Chaozhi, X. Guangzhi, Spectrochimica Acta, 45 A, 1029–1032 (1989)
24. J. L. Castro, J. C. Otero, J. I. Marcos, J. Raman Spectr. 28, 765–769 (1997)
25. Y. Fang, J. Raman Spectr., 30, 85–89 (1999)
26. V. P. Drachev W. Kim, V. P. Safonov, V. A. Podolskiy, N.S. Zakovryashin, E. N. Khaliullin, Vladimir M. Shalaev and R. L. Armstrong, J.of Mod. Opt, 2001 To be published
27. M. Moskovits, J. S. Suh, J. Am. Chem. Soc., 107, 6826–6829 (1985)
28. F. J. Adrian, J. Chem. Phys. **77**, 5302 (1982)
29. A. Campion, P. Kamphampati, Chem. Soc. Rev. **27**, 241 (1998)
30. J. R. Lombardi et al., J. Chem. Phys. **84**, 4174 (1986)
31. J. Lehman et al., J. Chem. Phys. **112**, 5428 (2000)
32. A. M. Michaels et al. J. Am. Chem. Soc. **121**, 9932 (1999)
33. T. Ya. Popova et al., Soviet Phys. JETP **30**, 243–247 (1970)